ZIBELINE INTERNATIONAL™ PUBLISHING

ISSN: 2521-0920 (Print)
ISSN: 2521-0602 (Online)
CODEN: MJGAAN

Malaysian Journal of Geosciences (MJG)

DOI: http://doi.org/10.26480/mjg.01.2026.01.08

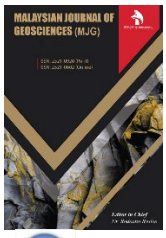

RESEARCH ARTICLE

GEOCHEMICAL FINGERPRINTS OF COASTAL SAND OF BENIN FORMATION, NIGER DELTA BASIN : IMPLICATION FOR PROVENANCE, MATURITY, WEATHERING AND PALEOREDOX CONDITIONS

Martins Ilevbare, Yusuf Olawale Agbaje*

Department of Geology, Afe Babalola University Ado - Ekiti, Ekiti State, Nigeria
Corresponding Author Email: yoagbaje@gmail.com

ARTICLE DETAILS

Article History:

Received 19 October 2025
Revised 27 November 2025
Accepted 15 December 2025
Available online 09 January 2026

ABSTRACT

The sand of the Benin formation in the Niger Delta basin of Nigeria was examined using X-ray fluorescence (XRF) and petrographic studies for its maturity, paleo-redox conditions, provenance and source area weathering. The paleo-redox conditions as revealed from the trace element ratios [(V/Cr: ~0.0025; V/Sc: ~0.03; Cr/Ni: ~3.52; V/Ni: ~0.009; U/Th: ~0.03; $V/(Sc)^3$: ~0.00052 and $V/(Ni+V)^2$: ~0.00028] as well from other geochemical fingerprints depict that the sediments strove in an oxidizing environment. The sand also had undergone substantial to intense chemical weathering (CIA: ~91.47; CIW: ~94.50; MIA: ~82.94; PIA: ~97.08) in a humid paleo- environment. The loss on ignition (LOI: ~7.33) investigated that significant amount of organic matter had been lost in the sample locations and that they had low sediment maturity (SiO_2/Al_2O_3: ~1.89). The provenance from the major oxides inferred that the samples were from felsic source rocks (Al_2O_3/TiO_2: ~27.67) with low clay content (ICV: ~0.34). The Quartz, Feldspar and Lithic (QFL) ternary diagram shows that the quartz type is sublithic-arenite and the petrographic studies indicate a compositionally mature sand. The correlation of the metallic oxides indicates an enrichment of silica and a depletion of other oxides signifying a common source for the sediments.

KEYWORDS

Coastal sand, sublithic-arenites, felsic source, geochemical fingerprint, intense chemical weathering

1. INTRODUCTION

Weathering is a fundamental geological phenomenon that entails the process of rock breakdown and alteration near the Earth's surface. To quantify and evaluate the extent of weathering in specific areas or on particular rocks, geologists employ weathering index. These indices offer quantitative measures that facilitate the comprehension of weathering processes and their impacts. Several weathering indices are employed in geology (Dengiz et al., 2019).

Provenance refers to the origin or source of sedimentary rocks or particles, as well as the processes and pathways involved in their transportation from the source area to their eventual deposition site (Omoruyi et al., 2022; Al-Momani et al., 2020). It involves the identification and characterization of the sediment source, which aids in deciphering the geologic history, paleogeography, and tectonic evolution of a region. In the context of sandstones, provenance refers specifically to the origin and sources of the sand grains that compose the rock, (Habboush and Jamar, 2009). On the contrary, petrography involves the detailed microscopic examination of sedimentary rocks to identify and quantify mineral types, grain sizes, grain shapes, and textural characteristics. Petrographic analysis assists in distinguishing between different source rock types and provides insights into the processes of weathering, transportation, and deposition, (Critelli and Martin-Martin, 2022; El-Hasan and Al-Malabeh, 2008).

Paleo-redox conditions refer to the prevailing oxygen levels in ancient Earth's oceans, lakes, and other geological environments. Understanding these conditions is crucial for reconstructing past environmental changes and their impact on the Earth's history, (Khoury, 2014 ; Khan et al., 2022).

This present study employs geochemical fingerprints with a view to provide insights into the source rocks of the sand, intensity of weathering, paleoclimate conditions during sediment formation and transportation, the oxygen level and redox state the depositional environment which can inform hydrocarbon exploration and potential reservoir characterization on a regional scale.

1.1 Study Area

The study area is Okomu National Park in Edo State. The study area is located between Latitude N 06° 22' 22.6 to N 6° 22' 19.8 and the Longitude is located between E 05° 14' 22.9 to E 05° 14' 21.6 (Figure 1). It is situated in an agricultural and fishery production area. The study area was accessible with major and minor roads.

Quick Response Code	Access this article online	
	Website: www.myjgeosc.com	**DOI:** 10.26480/mjg.01.2026.01.08

Cite the Article: Martins Ilevbare, Yusuf Olawale Agbaje (2026). Geochemical Fingerprints of Coastal Sand of Benin Formation, Niger Delta Basin: Implication For Provenance, Maturity, Weathering and Paleoredox Conditions. Malaysian Journal of Geosciences, 10(1): 01-08.

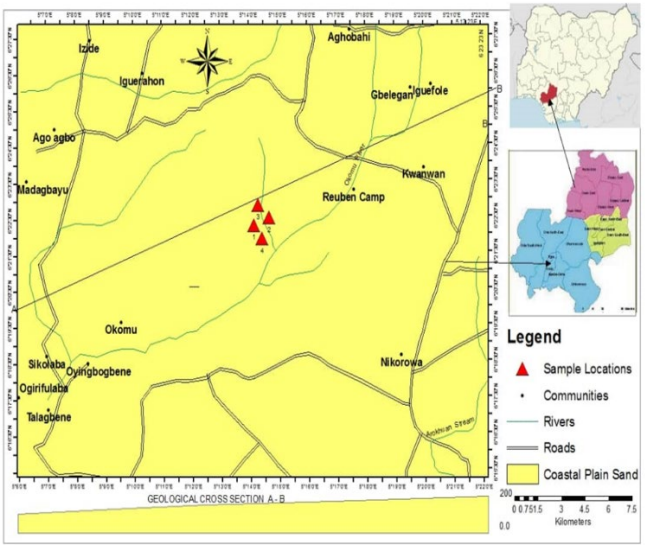

Figure 1: Geological Map of Okomu Sands, (Adopted from geological Survey of Nigeria, 1965).

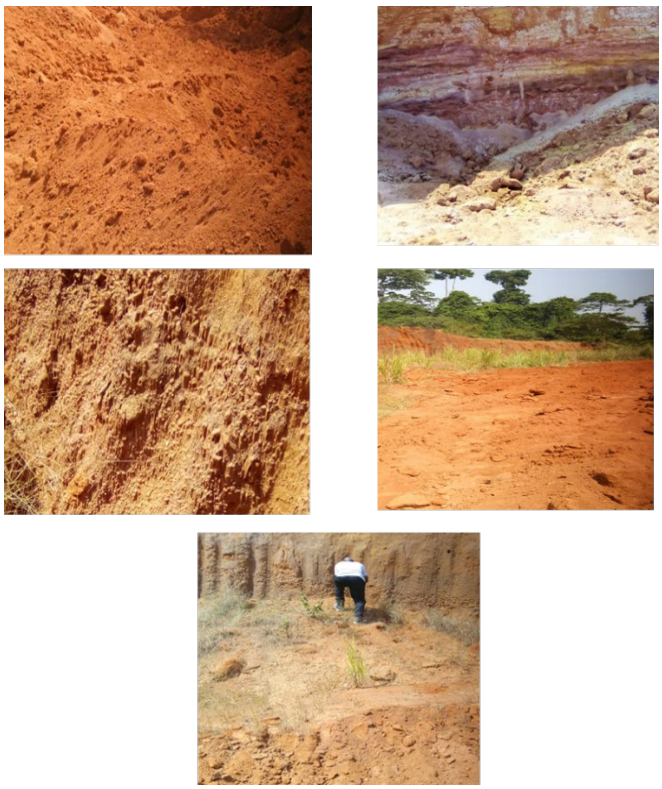

Figure 2: Field Photographs of Okomu Coastal Plain Sand

2. Materials And Methods

2.1 Materials

Forty (40) fresh sediment outcrop samples were collected from Okomu Forest Reserve in within the Benin formation, Niger Delta Basin. Chip and Grab sampling methods were adopted. Hammer, chisel, GPS, and sample bags were some of the materials used. The collected samples were analysed for major oxide and trace elements geochemistry and petrographic studies.

2.2 Methods

2.2.1 XRF for Major and Trace Elements Geochemistry

Ten (10) major oxides were analysed (SiO_2, TiO_2, Al_2O_3, Fe_2O_3, MgO, MnO, CaO, Na_2O, K_2O and P_2O_5) as well as twelve (12) trace elements (Ba, Rb, Sc, Ni, V, Cr, La, Zn, Cu, Th, U and Pb) were analysed for major oxides geochemistry using XRF analysis.

The procedure for XRF fusion method for analyzing major oxide is outlined as follows:

- 1.00g±0.0009g of milled sample is weighed. It is heated in an oven at 110°C for 1hour to determine H_2O^+. It is again placed in oven at 1000°C for 1hour to determine loss of Ignition (LOI).
- 10.00g ± 0.0009g of Claisse flux was added and fused in M4 Claisse fluxer for 23minutes.
- 0.2g of sodium trioxocarbonate IV (Na_2CO_3) plus mix plus the sample and the resulting mix was pre-oxidized at 700°C before fusion.
- Ultrapure flux is used (66.67% $Li_2B_4O_7$ + 32.83% $LiBO_2$) and a releasing agent Li-Iodide (0.5%LiI).
- Loss of Ignition (LOI) point is obtained by intensely heating a sample of the material at a specific temperature, to allow its gaseous contents to escape or by repeatedly adding oxygen until no mass change is observed.

In mineral industries and pro-processing, the LOI of the soil sample is approximately equal to the mass loss that the kiln, furnace or smelter will undergo (Madukwe and Obasi, 2016 ; Ilevbare and Imasuen, 2020).

2.2.2 Pressed Pellet method for Trace Element Analysis

- Weigh 8g ± 0.05 g of milled powder
- Mix thoroughly with 3 drops of wax binder
- Press pellet with pill press to 15-tonne pressure
- Dry in oven at 100°C for half an hour before analyzing (Okiotor and Ighodaro, 2020).

2.2.3 Thin Section Sample Preparation

Five (5) samples were analysed for thin section analysis. A thin section is useful for analysis in mineralogy. It provides invaluable insight and details into mineral compositions and rock formations.

Fresh loose samples were air dried for 24 hours, the samples were then impregnated with epoxy A and B and left to core for at least 24 hours, the cored sample is the trimmed to fit on a glass slide, the trimmed surface is lapped on the glass plate using water and silicon carbide 600grits, this is done so as to have a very smooth surface for bonding with the glass slide. One surface of the glass slide is also lapped and made smooth for bonding with the sample. The sample is then bonded to the glass slide using epoxy on the hot plate, this is allowed to bond for 24hours, the sample is then trimmed to 50µm on the glass slide using the cut-off saw machine and later transferred to the lapping plate and lapped to 30µm using silicon carbide and water, at 30micron the slide is ready for study under petrographic microscope counting method, which was also adopted was employed for the mineral grains compositional analysis, and the modal analysis, the method of counting over 300 points per thin section was used (Ingersoil et al., 1984 ; Tijani et al., 2010 ; Dickinson, 1970) .

3. Results And Discussion

The results have been represented using tables, charts and figures geared towards a comprehensive interpretation of the Data.

In the Table 1 of the major oxides and Figures (4.1-4.4), ten samples consisting of eleven oxides were analysed in percentages (%). SiO_2 ranged 54.82-63.40 (~57.11); Al_2O_3 ranged 11.20-31.23 (~27.50); Fe_2O_3 ranged 4.06-4.98 (~4.72); TiO_2 ranged 1.06-1.30 (~1.19); CaO ranged 1.50-1.75 (~1.46); P_2O_5 ranged 0.01-0.08 (~0.04); K_2O ranged 0.58-1.01 (~0.88); MnO ranged 0.03-0.08 (~0.07); MgO ranged 0.16-5.08 (~4.13); Na_2O ranged 0.06-0.90 (~0.78). The low concentration of Fe_2O_3, Al_2O_3 and TiO_2 (Figure 4.3) could be due to chemical disintegration under oxidizing conditions during weathering and diagenesis. It can also be observed that: SiO_2 > Al_2O_3 > Fe_2O_3 > MgO > CaO > TiO_2 > K_2O > Na_2O > MnO > P_2O_5 in abundance (fig. 3d). This data is needed in discussing the geochemistry of the coastal sand sourced from Okomu area.

Table 1: Major Oxides (%) Concentration and Weathering indices

Sample No.	SiO_2	Al_2O_3	Fe_2O_3	TiO_2	CaO	P_2O_5	K_2O	MnO	MgO	Na_2O	CaO*	CIA	CIW	PIA	MIA	ICV	LOI
OKU2	56.45	29.03	4.70	1.30	1.75	0.04	0.98	0.08	4.75	0.90	0.30	88.89	94.31	95.90	77.78	0.50	0.02
OKU4	56.70	30.22	4.06	1.23	1.66	0.05	1.01	0.07	5.08	0.87	0.25	89.67	92.27	96.31	79.34	0.45	0.05
OKU6	52.90	28.49	3.65	1.18	1.90	-	0.99	-	0.08	0.05	-	90.65	93.59	-	81.30	-	10.20
OKU8	56.38	29.24	3.65	1.04	1.45	0.01	0.94	0.01	0.46	0.28	0.44	91.63	94.41	97.52	83.26	0.27	10.55
OKU10	55.70	29.20	2.50	1.23	1.30	-	0.90	0.01	0.50	0.25	-	92.26	94.96	-	84.52	0.23	10.24
OKU12	54.54	27.70	2.82	0.55	1.20	0.03	0.85	0.01	0.55	0.47	0.20	91.66	94.31	97.57	83.32	0.23	0.02
OKU14	50.90	30.47	3.65	1.20	1.90	-	0.99	-	0.08	0.05	-	91.20	94.00	-	82.40	-	11.30
OKU16	56.40	29.22	3.65	1.04	1.45	0.01	0.95	0.01	0.45	0.28	0.33	91.60	94.41	97.89	83.20	0.27	10.20
OKU18	55.68	29.20	2.50	1.22	1.30	-	0.90	0.01	0.50	0.25	-	92.26	94.96	-	84.52	-	10.55
OKU20	54.50	27.72	2.84	0.55	0.20	0.05	0.85	0.01	0.55	0.45	0.33	94.87	97.71	97.28	89.74	0.20	10.24
AVER.	55.02	29.05	3.40	1.05	1.31	0.03	0.94	0.03	1.30	0.39	0.31	91.47	94.50	97.08	82.94	0.34	7.33

CIW – Chemical index of weathering; CIA – Chemical index of alteration; PIA – plagioclase index of alteration; MIA – Mineral index of alteration

For the upper band composite bar chart (Fig. 3a), it shows that SiO_2 is predominant in the coastal plain sands as compared to Al_2O_3 (30ppm) with SiO_2 having ppm of about 50 to 60 ppm.

For the middle band composite bar chart (Fig. 3b), it shows that Iron oxide and Magnesium oxides are predominant or most abundant. For the Middle Band Composite Bar Chart, it shows that Silicon oxide and Aluminium oxide are the most abundant.

For the lower band composite bar chart (Fig. 3c), it shows the lowest major oxides in the samples of the coastal plain sands with MnO (0.08ppm) being lower as compared to P_2O_5 (0.06ppm).

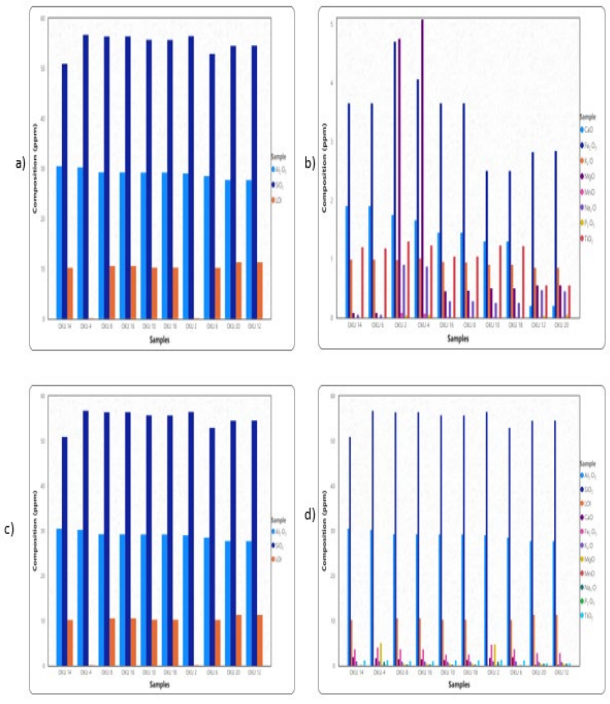

Figure 3(a - d): (a) Upper band, composite bar chart (Al_2O_3, SiO_2, LOI) **(b)** Middle band composite bar chart (CaO, Fe_2O_3, K_2O, MgO, MnO, Na_2O, P_2O_5, TiO_2) **(c)** Lower band composite bar chart (MnO, P_2O_5) and **(d)** Composite bar chart of all components (major oxides, LOI)

3.1 Major Elements Geochemistry

The SiO_2 content (~55.02) can be associated with the presence of quartz particles: the highest value for all samples refers to the higher sand fraction in particle size distribution analysis and higher quartz content in mineral composition which is indicated by the values of this study (Table 4.1). Quartz is well enriched in felsic igneous rocks. SiO_2 strongly resists weathering because it is mainly contained in quartz minerals (Nzeukou et al., 2021).

Alumina (Al_2O_3) reflects the presence of aluminosilicates (~29.05). Al_2O_3 is mainly less resistant to weathering because it is contained in the clay minerals; a high content of Al_2O_3 indicates a high content of clay minerals (Dengiz et al., 2019); the values of Al_2O_3 recorded in this study indicate low clay content (Table 1).

Iron (Fe_2O_3) is related to the presence of hematite (~3.40). Fe_2O_3 being > 2 is probably responsible for the extreme changes in colour of the shales from pink, yellow to red and the deposition of iron minerals (Nzeukou et al., 2021). Some samples had no record of P_2O_5, thus were not found and thus, the CaO* and PIA for that location could not be calculated (Table 4.1).

CaO* was not recorded in four locations due to the absence of P_2O_5 in corresponding locations. CaO* represents the CaO contained only in the silicate fraction and is corrected for carbonate

and apatite content. It is based on the assumption for CaO* that the molar CaO/Na_2O ratio of silicates is <1 as seen in this study where CaO* (~0.31) reflecting low calcite content in the sands collected (Table 1).

3.2 Provenance and Maturity

The geochemical attributes of elements and their ratios (major and trace elements) in clastic sedimentary rocks are invaluable for construing provenance (Oti and Nwachukwu, 2021). The major oxide ratios (Table 2) are very useful tools in the interpretation of provenance and maturity of sediments. The averages of SiO_2/Al_2O_3, Fe_2O_3/K_2O, Al_2O_3/TiO_2, K_2O/Al_2O_3 are 1.89, 3.62, 27.67 and 0.03 respectively with Al_2O_3/TiO_2 being fairly high and K_2O/Al_2O_3 being extremely low, (Table 2).

Table 2: Significant ratios of major oxides of Okomu sand

Sample No	SiO_2/Al_2O_3	Fe_2O_3/K_2O	Al_2O_3/TiO_2	K_2O/Al_2O_3
OKU2	1.94	4.80	22.33	0.03
OKU4	1.88	4.02	24.57	0.03
OKU6	1.86	3.70	24.14	0.03
OKU8	1.93	3.88	28.12	0.03
OKU10	1.91	2.78	23.74	0.03
OKU12	1.97	3.32	50.36	0.03
OKU14	1.67	3.69	25.39	0.03
OKU16	1.93	3.84	28.10	0.03
OKU18	1.91	2.78	23.93	0.03
OKU20	1.97	3.34	50.40	0.03
AVERAGE	1.89	3.62	27.67	0.03

3.3 Provenance

Al_2O_3 was greatly enriched in the soil samples compared to TiO_2 (Table 1). Sediments from mafic rocks have Al_2O_3/TiO_2 ratio <14 while sediments from felsic rocks ranged from 19-28; also reported was a range of 3–8, 8–21, and 21–70 for mafic-igneous, intermediate, and felsic sources respectively (Ilevbare and Omoruyi, 2020). The average reported in Table 4.2 indicated here (22.33-50.40; ~27.67) in this study infers that the sand was strictly of felsic source (with no mixed provenance).

Fe_2O_3/K_2O (2.78-4.80; ~3.62) showed that there was relatively higher deposition of iron oxide compared to potassium oxide (Table 2); however, this low ratio shows that the rock originated from felsic igneous rocks such as granite and they also indicate an oxidizing environment (Liu et al., 2021). According to the presence of haematite cements denotes an oxidizing environment thus suggesting that a humid climate prevailed in the area during the period of deposition (Adeila et al., 2019).

K_2O/Al_2O_3 (~0.03) indicates burial diagenesis was probable (Ghosh et al., 2019). K_2O was not greatly enriched in the soil samples compared to Al_2O_3 (Table 1).

3.4 Maturity of the Sediments

Maturity of sand can be reflected by the SiO_2/Al_2O_3 index. High ratios indicate mineralogically mature sands, while low ratios represent chemically immature sands (Haque and Roy, 2019). With increasing sediment maturity, quartz survives preferentially to feldspars, mafic minerals and lithics (Madukwe and Obasi, 2016). Low values of K_2O/Al_2O_3 indicate low sediment maturity (Haque and Roy, 2019). K_2O/Al_2O_3 values of ~0.03 in this study (Table 2) rightly indicate so.

The index compositional variation (ICV) can determine the original character and maturity of sediments, as well as the climatic conditions. In minerals that are high in weathering intensity and decreases in more stable minerals (less weathered minerals) show the highest tends of the ICV. The ICV (0.34 ave.) from this study indicates that the sediments are majorly non-clay, (Table 1).

The compositional maturity of the coastal plain sand (table 3) with angular to subangular grains that are monocrystalline and polycrystalline. The monocrystalline samples were less and had rounded to subrounded boundaries. Also observed was that the ratio of polycrystalline to monocrystalline was higher in all samples (the least being 54:44). The polycrystalline grain size is affected by a number of factors such as grain size, type of material, processing conditions and presence of impurities. However, materials with finer polycrystalline grain size will have better properties such as ductility, strength, toughness, stiffness than those with a coarser grain size.

In all, the compositional maturity table (Table 3), revealed that the sands were compositionally mature (91-93% qtz).

Table 3: Compositional Maturity of the Coastal Plain Sands

Sample ID	Quartz (grain type)	Angular Boundary	No. of Count	Ratio of Polycrystalline to Monocrystalline	Compositional Maturity
OKU2	Polycrystalline Monocrystalline	Angular to Subangular Rounded to subrounded	54 44	54:44	Super mature (=93%Qtz)
OKU4	Polycrystalline Monocrystalline	Angular to Subangular Rounded to subrounded	60 47	60:47	Super mature (=92% qtz)
OKU6	Polycrystalline Monocrystalline	Angular to Subangular Rounded to subrounded	57 45	57:45	Super mature (=91% qtz)

Table 3 (cont): Compositional Maturity of the Coastal Plain Sands					
OKU10	Polycrystalline Monocrystalline	Angular to Subangular Rounded to subrounded	63 52	63:52	Super mature (=92% qtz)
OKU12	Polycrystaline Monocrystaline	Angular to Subangular Rounded to subrounded	58 47	58:57	Super mature (=93% qtz)

The depositional conditions of angular to subangular grain sizes can provide valuable insights into the processes and environments in which sedimentary rocks were formed.

Angular grains are typically observed near the source area of sediment, where erosion and transportation processes have not had enough time to round them. The presence of angular to subangular grains suggests that deposition occurred relatively close to the original sediment source. Angular grains can be indicative of high-energy depositional environments, such as steep slopes, fast-flowing rivers, or nearshore areas exposed to strong wave action. In these energetic settings, sediment transport is more likely to occur without extensive rounding or abrasion, (Ilevbare and Imasuen, 2020).

The preservation of angular to subangular grains suggests rapid deposition and minimal transportation. When sediments are quickly deposited, there is less time for rounding and sorting processes to occur, leading to the retention of angularity. Angular to subangular grain sizes are often associated with specific sedimentary structures, such as gravel bars, alluvial fans, or debris flows. These structures are commonly formed by fast-moving sediment-laden fluids or mass wasting events, which result in the deposition of relatively coarse, angular sediments. In some cases, angular to sub-angular grains may indicate reworking or disturbance of previously deposited sediments. Some sedimentary deposits affected by tectonic activity or glaciation can be disrupted, resulting in the preservation of angular grains during subsequent deposition, (Ilevbare and Omorogieva, 2020).

In addition to depositional environment, the degree of rounding can also be used to infer the age of sediment. In general, older sediments tend to be more rounded than younger sediments. This is because older sediments have had more time to be transported and abraded. The degree of rounding can also be used to infer the source of sediment. For example, sediments that are derived from bedrock that is composed of angular rocks will tend to have angular grains. Sediments that are derived from bedrock that is composed of rounded rocks will tend to have rounded grains, (Ilevbare and Omodolor, 2020).

Grain sizes that are rounded to sub-round also provide important information about the depositional conditions of sedimentary rocks. Rounded to sub-rounded grains are typically observed in sediments that have undergone significant transportation. The extent of rounding indicates the distance travelled by the sediment from its source. The longer the transportation distance, the more rounded the grains tend to become due to abrasion and attrition during transport. Rounded to sub-rounded grain sizes are commonly associated with low to moderate energy depositional environments, such as meandering rivers, deltas, beaches, or offshore areas. In these settings, the energy levels are relatively lower compared to high-energy environments, allowing sediment to be transported over longer distances and undergo rounding processes. Rounded to sub-rounded grain sizes are commonly found in sedimentary rocks that were deposited in fluvial (river), lacustrine (lake), and marine environments. They are also found in glacial deposits, such as till and outwash, (Ilevbare and Omodolor, 2020).

The rounding of grains requires time for abrasion and attrition to occur. Sediments with rounded to sub-rounded grains suggest longer periods of deposition, allowing for sufficient time and transportation to achieve the observed degree of rounding. Rounded to sub-rounded grains are often observed in moderate to fine-grained sediments, where the grains are more susceptible to abrasion during transport. Coarser grains may retain some angularity even after extended transport. Rounded to sub-rounded grains can indicate relatively stable or quiescent depositional environments. In these settings, sediment is not constantly reworked or disturbed, allowing grains to undergo prolonged rounding processes, (Maduke and Obasi, 2016).

Al_2O_3 and SiO_2 correlates as a negative linear relationship and negatively poor correlated (figure 4; Table 4).

Table 4: Al_2O_3 and SiO_2 Correlation result		
Oxides	*Al_2O_3*	*SiO_2*
Al_2O_3	1	
SiO_2	-0.045373	1

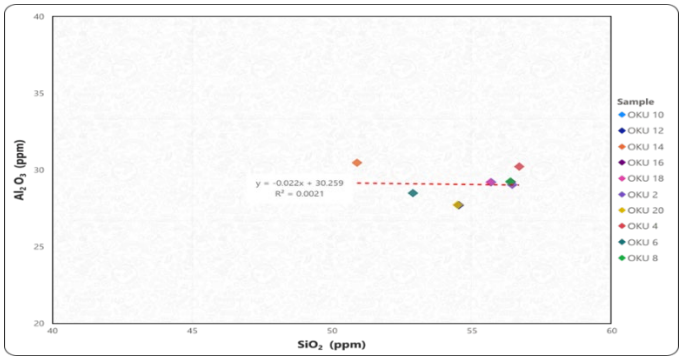

Figure 4: Correlation cross plot of Al_2O_3 and SiO_2

Correlation strength: 0 - 0.29 (Poor); 0.3 - 0.69 (Weak); 0.7-1.0 (Strong)

Fe_2O_3 and Al_2O_3 correlates as a positive linear relationship and positively weak (figure 5; Table 5).

Table 5: Al_2O_3 and SiO_2 Correlation result		
	Fe_2O_3	*Al_2O_3*
Fe_2O_3	1	
Al_2O_3	0.393797	1

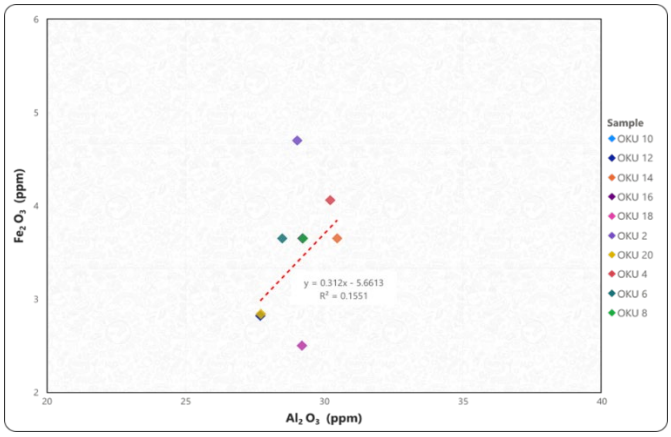

Figure 5 : Correlation cross plot of Fe_2O_3 and Al_2O_3

Fe_2O_3 and SiO_2 correlates as a positive linear relationship and positively poor (Figure 6; Table 6)

Table 6: SiO_2 and Fe_2O_3 Correlation result		
	SiO_2	*Fe_2O_3*
SiO_2	1	
Fe_2O_3	0.120424	1

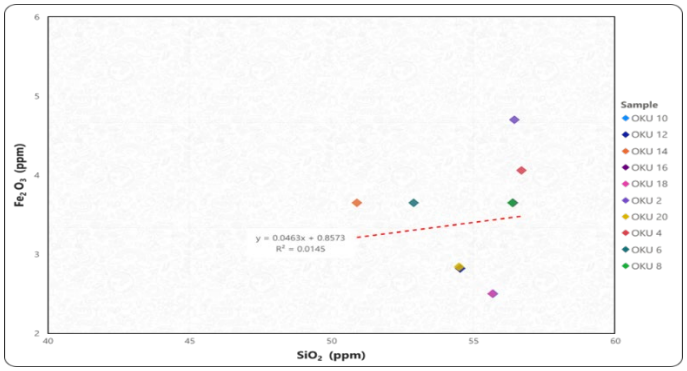

Figure 6: Correlation cross plot of SiO_2 and Fe_2O_3 Correlation

Al_2O_3 and TiO_2 correlates as a positive linear relationship and positively poor (figure 7; Table 7) For all the coastal plain sands analysed, the negatively correlated oxides (figure 4) show the changes brought about by weathering through the enrichment silica content and the depletion of iron and titanium oxides and typifies a felsic source rock. This finding from the correlation of the major oxides authenticates the results of the source area weathering from the weathering index with evidence that the sediments have undergone chemical weathering. The positively correlated oxides, (figures 5, 6 and 7) are an indication of a common source area.

Table 7: TiO_2 and SiO_2 Correlation		
	TiO_2	*SiO_2*
TiO_2	1	
SiO_2	0.101212	1

Figure 7. Correlation cross plot of TiO_2 and SiO_2

3.5 Chemical Weathering

For the weathering index in Table 1, the chemical index of alteration (CIA) ranged 88.89 - 94.87 with an average of 91.47; the chemical index weathering (CIW) ranged 92.27-97.71 with an average of 94.50; the plagioclase index of alteration (PIA) ranged 95.90-97.89 with an average of 97.08 and the mineralogy index of alteration (MIA) ranged 77.78-89.74 with an average of 82.94.

According to Nesbitt and Young, 1982, weathering at the incipient stage is indicated by CIA (30 - 55), weathering at the intermediate stage, CIA (51-85) and weathering at the advanced stage, CIA (> 85). The CIA spectra of 50–60 indicate low chemical weathering, 60–80 suggests moderate chemical weathering (in cool and/or arid climate), and 80–100 implies intensive chemical weathering (McLennan et al., 1993; Ejeh, 2021). For the coastal plain sand studied, CIA (91.47 ave.) suggests an advanced stage, intense chemical weathering.

Chemical Index of Weathering (CIW) of 50 for unweathered upper continental crust to roughly 100 for materials that have undergone substantial weathering with the full elimination of alkali and alkaline-earth elements (McLennan et al., 1993 ; Mongelli et al., 1996). The coastal plain sands with a CIW of 94.50 (92.27-97.71) signifies that the sand had undergone substantial weathering.

Unweathered plagioclase has PIA value of 50 while Phanerozoic samples have PIA value of 79, PIA in this study had an average of 97.08 (95.90-97.89) indicating intense weathering of Phanerozoic samples (Fedo et al., 1995).

The mineralogical index of alteration (MIA), incipient (0–20%), weak (20–40%), moderate (40–60%) and intense to extreme (60–100%) degree of weathering (Omoruyi et al., 2022). This study (Table 1) had MIA average of 82.94 with characteristically intense to extreme weathering of the sands. Therefore, the CIA, PIA, CIW and MIA indicate that the sands had an advanced stage/intense to extreme chemical weathering.

3.6 Trace Elements Geochemistry

In this study, the concentration of these redox-sensitive elements, such as V, Ni, Cu, Cr Mo, Ba, Rb, Zn, Sc, La, Th, U and Pb (Table 4.3) were sensitive indicators of prevalence paleo-conditions. For example, the concentration of vanadium (V) and nickel (Ni) as well as their ratios provide a means of determining the degree of anoxia during deposition. Vanadium is usually enriched in comparison with nickel in anoxic marine environments. This is due to strong activities of the sulphate reduction bacteria in this environment and greater relative stability of vanadyl versus nickel porphyrin complexes. The reverse is the case under normal oxic conditions (Olajubaje et al., 2018).

The relative abundance of trace elements and oxides in sediment is controlled by sedimentation rate, terrigenous influx, biogenic influx, hydrothermal input, diagenesis and, ultimately, weathering. Their enrichments can lead to understanding of their paleo-depositional and paleo redox setting, as well as the paleoclimate.

The trace element concentration in ppm (Table 8) of ten (10) trace elements analysed and their values are given in ppm: Ba (650-841; ~817), Cr (87-122; ~109), Ni (26-40; ~31); Sc (6-9; ~8), Rb (6-8; ~8), Pb (6-14; ~11), Cu (22-29; ~32), V (0.23-0.34; ~0.27), Th (5.12-6.50; ~5.86), Zn (210-240; ~217), La (0.20-0.28; ~0.22) and U (0.17-0.22; ~0.20).

Table 8: Trace Elements Concentration (ppm).												
Sample Number	Ba	Cu	Cr	Ni	Sc	Rb	V	La	Th	U	Zn	Pb
OKU2	841	22	103	28	8	6	0.24	0.20	5.15	0.17	240	6
OKU4	650	24	87	40	6	8	0.23	0.22	6.10	0.20	220	10
OKU6	663	28	100	32	8	8	0.28	0.20	5.12	0.21	210	11
OKU8	673	28	112	32	8	8	0.33	0.22	5.74	0.20	210	10
OKU10	663	27	110	31	9	6	0.34	0.22	5.59	0.20	214	13
OKU12	671	28	120	28	6	8	0.28	0.20	6.22	0.20	220	13
OKU14	666	29	105	30	9	8	0.20	0.24	6.20	0.22	212	12
OKU16	671	26	112	33	9	8	0.33	0.22	5.54	0.20	213	13
OKU18	658	26	114	29	8	8	0.25	0.28	6.40	0.22	210	14

Table 8 (cont): Trace Elements Concentration (ppm).												
OKU20	674	26	122	26	9	8	0.23	0.22	6.50	0.20	222	10
AVERAGE	817	32	109	31	8	8	0.27	0.22	5.86	0.20	217	11

High concentrations of Ba even as seen in the results of this study indicate the presence of marine depositional environment (Zhang et al., 2021). According to this study, Ni concentrations larger than 200 ppm signs of mafic or ultramafic provenance. For this study, Ni with an average of 31 indicates that the Okomu sands are of felsic origin (Gao et al., 2020).

When Cr is greater than 150ppm in abundance, it is an indication of mafic or ultramafic provenance. The highest recorded value of Cr in this study was 122 ppm indicating a felsic provenance relative to the above conditions (Omoruyi et al., 2022).

3.7 Paleo-redox conditions of the Sediment

Despite the usefulness of the redox-sensitive trace elements in determining paleo-redox conditions, the invaluable need for cautious use and in a relative sense (Fu et al., 2019). This is because of the problems associated with comparing their ratios directly to the threshold suggested in previous studies. Trace elements such as Cr, Th, U, V, Ni, and Mn are redox sensitive and useful in the reconstruction of paleo-redox conditions of the depositional environment (Matthew et al., 2019). Trace composition and elements ratio (V/Cr, V/Sc, Cr/Ni, V/Ni and U/Th, $V/(Sc)^3$ and $V/(Ni+V)^2$) have been used for determining paleo-redox conditions (Jones and Manning, 1994).

In the ratios of the trace elements, (Table 9), V/Cr ($1.9x10^{-3}$- $3.1x10^{-3}$; $\sim 2.5x10^{-3}$), U/Th (0.03-0.04; ~0.03), Cr/Ni (2.18-3.68; ~3.52), V/Ni (0.005-0.01; ~0.009), V/Sc (0.02-0.05; ~0.03), $V/(Ni+V)^2$ ($2.7x10^{-4}$-$1.3x10^{-3}$; $\sim 2.8x10^{-4}$), $V/(Sc)^3$ ($2.7x10^{-4}$-$1.1x10^{-3}$; $\sim 5.2x10^{-4}$).

The ratio of V/Cr to decipher paleo-redox conditions and stated that ratio values of <2, 2-4.25, and >4.25 represented oxic, dysoxic, and suboxic and anoxic conditions, respectively (Jones and Manning, 1994). Similarly, the V/Cr ratio has been used as a paleo-oxygenation indicator in a number of studies. In a similar vein, values of V/Cr >2 represent anoxic depositional conditions, whereas values below 2 are indicative of more oxidizing conditions (Olajubaje et al., 2018). The V/Cr ratios of the examined samples are far below 2 (~ 0.0025) and therefore indicate the oxic depositional setting (Table 4.9).

The ratio of U/Th to distinguish between oxic (<1.25) and suboxic to anoxic (>1.25) settings. The U/Th ratios of the samples from Okomu community was 0.03-0.04 (~ 0.03) rightly indicating an oxidizing paleo-environment (Jones and Manning, 1994).

Table 9: Significant ratios of the trace elements of Okomu Sands

Sample No	V/Cr	U/Th	Cr/Ni	V/Ni	V/Sc	$V/(Ni+V)^2$	$V/(Sc)^3$
OKU2	$2.3x10^{-3}$	0.03	3.68	0.008	0.03	$3.0x10^{-4}$	$4.7x10^{-4}$
OKU4	$2.6x10^{-3}$	0.03	2.18	0.005	0.04	$1.4x10^{-4}$	$1.1x10^{-3}$
OKU6	$2.8x10^{-3}$	0.04	3.13	0.009	0.04	$2.7x10^{-4}$	$5.5x10^{-4}$
OKU8	$2.9x10^{-3}$	0.03	3.50	0.01	0.04	$3.2x10^{-4}$	$6.4x10^{-4}$
OKU10	$3.1x10^{-3}$	0.04	3.55	0.01	0.04	$3.5x10^{-4}$	$4.7x10^{-4}$
OKU12	$2.3x10^{-3}$	0.03	4.30	0.01	0.05	$3.5x10^{-4}$	$1.3x10^{-3}$
OKU14	$1.9x10^{-3}$	0.04	3.50	0.007	0.02	$2.2x10^{-4}$	$2.7x10^{-4}$
OKU16	$2.9x10^{-3}$	0.04	3.40	0.01	0.04	$3.0x10^{-4}$	$4.5x10^{-4}$
OKU18	$2.2x10^{-3}$	0.03	3.93	0.009	0.03	$3.0x10^{-4}$	$4.9x10^{-4}$
OKU20	$1.9x10^{-3}$	0.03	4.69	0.009	0.03	$3.3x10^{-4}$	$3.2x10^{-4}$
AVERAGE	$2.5x10^{-3}$	0.03	3.52	0.009	0.03	$2.8x10^{-4}$	$5.2x10^{-4}$

According to the concentration of vanadium (V), and nickel (Ni) as well as their ratios provide a means of determining the degree of anoxia during deposition. Vanadium is usually enriched in comparison with Ni in anoxic marine environments. In this study, the reverse is the case as nickel is more enriched than vanadium in the soil samples which imply that an oxic setting was prevalent. In this investigation, V/Ni ranged 0.0002-0.003 with an average of 0.0008 indicating oxidizing conditions in the shale samples studied (Olajubaje et al., 2018).

Applying the standards used in previous work: $V/(Ni+V)^2$ ($2.7x10^{-4}$-$1.3x10^{-3}$; $\sim 2.8x10^{-4}$), being less than 0.46 and $V/(Sc)^3$ ($2.7x10^{-4}$-$1.1x10^{-3}$; $\sim 5.2x10^{-4}$), being less than 9.1 both signify an oxic depositional state, (Jones and Manning, 1994). The application of trace element composition ratios: V/Cr, V/Ni, U/Th, $V/(Ni+V)^2$, $V/(Sc)^3$ as proxies for paleo-redox conditions of the sediments obtained from the Okomu community of this research work all revealed oxic depositional setting.

3.8 QFL Ternary Diagram

The coastal plain sands from the ternary plot (figure 8) are of sublitharenite with quartz percentage been > 90%.

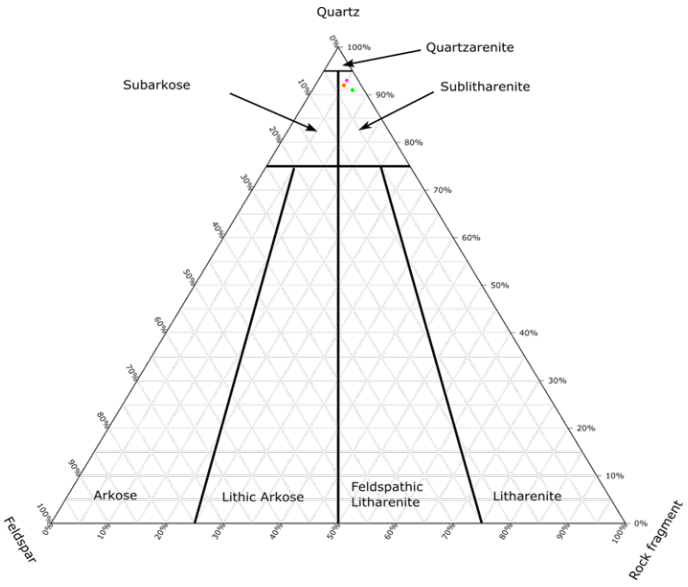

Figure 8: QFL ternary plot of coastal plain Sands

3.9 Petrographic Studies for the Coastal plain Sands

The photomicrograph (figure 9) of the sand of the studied locations from the petrographic examination was found to be composed of Quartz (Q), Matrix element (M), Feldspar (F) and Rock fragment (RF). This mineral composition identification can be used for the modal composition of the costal sand, from which the textural, compositional and mineral maturity index are also determined.

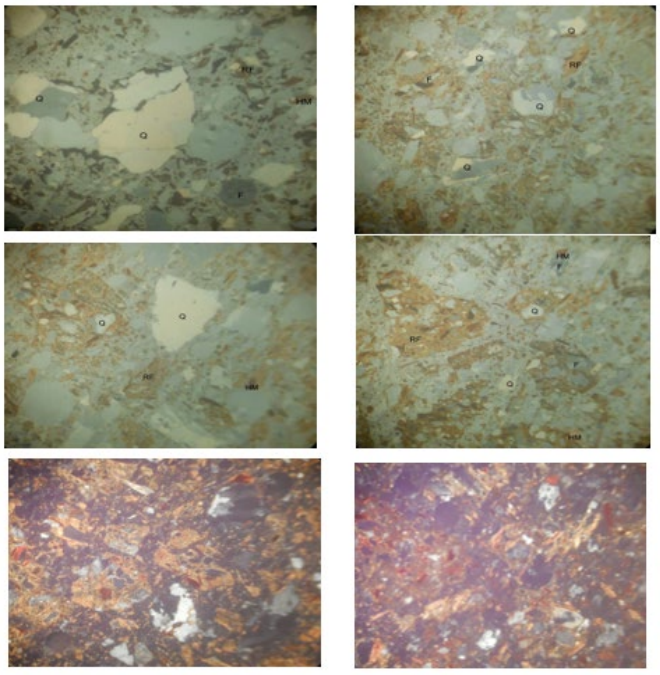

Figure 9: Microphotogram for Petrographic Studies

The Thin Section Photographs (Figure 9) the Q, F, RF and HM are quartz, feldspar, rock fragments and heavy minerals, respectively.

4. Conclusion

The following conclusions were drawn from the Geochemical discrimination of the coastal plain sand at Okomu Reserve in Benin Formation, Niger Delta Basin:

- The quartz type of the coastal sand is of sub-litharenites, felsic source rock in an oxidizing paleo-environment.
- Weathering occurred in a humid climate and the sands had undergone substantial, advanced stage/intense to extreme chemical weathering.
- The correlation of the major oxides indicates that the provenance of the coastal plain sand was from a common source rock.

Statement Of Interest

The authors declare that there is no significant competing financial, professional, or personal interests that might have influenced the performance or presentation of the work described in this manuscript.

References

Adiela, U.P., Jackson, C.A., and Moses, A., 2019. Sedimentology and depositional environment of Ajali Sandstone, Anambra Basin, Southern Nigeria. ResearchGate. Retrieved from https://www.researchgate.net/publication/338210042

Al-Momani, T., Alqudah, M., and Dwairi, M.E.A., 2020. Mineralogical and geochemical characterisation of Jarash kaolinitic clay, northern Jordan. Jordan Journal of Earth and Environmental Sciences, 11(4), Pp. 272–287.

Critelli, S., and Martin-Martin, M., 2022. Provenance, paleogeographic and paleotectonic interpretations of Oligocene–Lower Miocene sandstones of the western–central Mediterranean region: A review. Journal of Asian Earth Sciences: X, Article ID 100124.

Dengiz, O., Tunçay, T., Bayramin, I., Kilic, S., and Baskan, O., 2019. Chemical weathering indices applied to soils developed on old lake sediments in a semi-arid region of Türkiye. Eurasian Journal of Soil Science. https://doi.org/10.18393/ejss.499122

Dickinson, W.R., 1970. Interpreting detrital modes of greywacke and arkose. Sedimentary Petrology Journal, 40, Pp. 695–707.

Ejeh, O.I., 2021. Geochemistry of rocks (Late Cretaceous) in the Anambra Basin, SE Nigeria: Insights into provenance, tectonic setting, and paleo-conditions. Heliyon, Article ID e08110. https://doi.org/10.1016/j.heliyon.2021.e08110

El-Hasan, T., and Al-Malabeh, A., 2008. Geochemistry, mineralogy and petrogenesis of El-Lajjoun Pleistocene alkali basalt of central Jordan. Jordan Journal of Earth and Environmental Sciences, 1(2), Pp. 53–62.

Fedo, C.M., Nesbitt, H.W., and Young, G.M.. 1995. Unraveling the effects of K-metasomatism in sedimentary rocks and paleosols with implications for paleo-weathering conditions and provenance. Geology, 23, Pp. 921–924.

Fu, X., Wang, J., Song, C., Wang, Z., Zeng, S., and Wang, D., 2019. The Permian–Triassic transition in ocean-island settings: Environmental disturbances and new high-resolution carbon-isotope record from the Qiantang Basin, NW China. Palaeogeography, Palaeoclimatology, Palaeoecology, 522, Pp. 40–51.

Gao, X., Zhang, X., and Zhu, X., 2020. Provenance and tectonic implications of Palaeozoic strata in the South Yellow Sea Basin, China, revealed from Borehole CSDP-2. Journal of Ocean University of China, 19, Pp. 536–555.

Ghosh, S., Mukhopadhyay, J., and Chakraborty, A., 2019. Clay mineral and geochemical proxies for intense climate change in the Permian Gondwana rock record from eastern India. Research Article, Article ID 8974075. https://doi.org/10.34133/2019/8974075

Habboush, M.A., and Jarrar, G.H., 2009. Petrology and geochemistry of the metasediments of the Janub metamorphic suite, southern Jordan: Implications for geothermobarometry and economic potential. Jordan Journal of Earth and Environmental Sciences, 2(1), Pp. 7–17.

Haque, M.M., and Roy, M.K., 2019. Sandstone–shale geochemistry of Miocene Surma Group in Bandarban Anticline, SE Bangladesh: Implications for provenance, weathering, and tectonic setting. Earth Sciences, 9(1), Pp. 38–51. https://doi.org/10.11648/j.earth.20200901.15

Ilevbare, M., and Imasuen, O.I., 2020. Sedimentology and maturity of Ajali Formation, Benin flank, Anambra Basin, Nigeria. Ife Journal of Science, 22(1), Pp. 123–135.

Ilevbare, M., and Omorogieva, O.M., 2020. Sedimentary petrology, paleoclimatic and tectonic settings of Maastrichtian

sediments, western flank of Anambra Basin, Nigeria. Nigeria Research Journal of Engineering and Environmental Sciences, 5(2), Pp. 938–949.

Ilevbare, M., and Omoruyi, D.I., 2020. Trace elements and major oxides characteristic of Ajali Sandstone, southwest Anambra Basin, Nigeria. Nigeria Research Journal of Engineering and Environmental Sciences, 5(2), Pp. 737–742.

Ilevbare, M., and Omodolor, H.E., 2020. Ancient depositional environment, mechanism of deposition and textural attributes of Ajali Formation, western flank of Anambra Basin, Nigeria. Case Studies in Chemical and Environmental Engineering, 2, Pp. 1–8.

Ingersoll, R.V., Bullard, T.F., Ford, R.L., Grim, J.P., Pickle, J.D., and Sares, S.W., 1984. The effects of grain size on data modes: A test of the Gazzi–Dickinson point-counting method. Sedimentary Petrology Journal, 46, Pp. 620–632.

Jones, B., and Manning, D.A.C., 1994. Comparison of geochemical indices used for the interpretation of palaeoredox conditions in ancient mudstones. Chemical Geology, 114, Pp. 111–129.

Khan, S.A., Dar, S.A., Khan, K.F., and Karim, Y., 2022. Geochemical characteristics of Early Cambrian phosphate-bearing sedimentary rocks from the Mussorie Syncline, India: Implications for paleo-redox conditions. Geosystems and Geoenvironment, 1(3), Article ID 100046.

Khoury, H.N., 2014. Geochemistry of surficial uranium deposits from central Jordan. Jordan Journal of Earth and Environmental Sciences, 6(3), Pp. 11–22.

Liu, W., Liu, X., Xie, Y., and Zhao, Y., 2021. Detrital zircon U-Pb age and geochemical constraints on the provenance and tectonic setting of the Carboniferous to Permian sandstones in the Qaidam Basin, NW China. Arabian Journal of Geosciences, 14(7), 446.

Madukwe, H.Y., and Obasi, R.A., 2016. Geochemistry, classification and maturity of the sandstone facies of the Abeokuta Formation, southwestern Nigeria. European Journal of Basic & Applied Sciences, 3(2), Pp. 125–138.

Matthew, R.S., Jessica, H.W., Timothy, W.L., and Matthew, O.C., 2019. Marine redox conditions through the late Palaeozoic icehouse–greenhouse transition. Palaeogeography, Palaeoclimatology, Palaeoecology.

McLennan, S.M., Hemming, S., McDaniel, D.K., and Hanson, G.M., 1993. Geochemical approaches to sedimentation, provenance, and tectonics. In M.J. Johnsson and A. Basu (Eds.), Processes Controlling the Composition of Clastic Sediments (Vol. 284, Pp. 21–40). Geological Society of America Special Papers.

Mongelli, G., Cullers, R.L., and Muelheisen, S., 1996. Geochemistry of Late Cretaceous–Oligocene shales from the Varicolori Formation, southern Apennines, Italy: Implications for mineralogical, grain-size control and provenance. European Journal of Mineralogy, 8, Pp. 733–754.

Nesbitt, H.W., and Young, G.M., 1982. Formation and diagenesis of weathering profiles. Journal of Geology, 97, Pp. 129–147.

Nzeukou, N.A., Tsozué, D., Kagonbé, P.B., Balo, M.A., Fankam, D., Ngosi, S., Nkoumbou, C., and Fagel, N., 2021. Clayey soils from Boulgou (North Cameroon): Geotechnical, mineralogical, chemical characteristics and properties of their fired products. SN Applied Sciences, 3, Article ID 551. https://doi.org/10.1007/s42452-021-04541-4

Okiotor, M.E., and Ighodaro, E.J., 2020. Geotechnical appraisal of the Mamu Shales exposure around Igodor in the Benin flank of Anambra Basin. Journal of Applied and Environmental Management, 24(3), Pp. 489–493.

Olajubaje, T.A., Akande, S.O., Adeoye, J.A., Adekeye, O.A., and Friedrich, C., 2018. Depositional environments and geochemical assessments of the Bende–Ameki Formation potential as petroleum source rocks in the Ogbunike Quarry, southeastern Nigeria. European Scientific Journal, 14(27), Pp. 157–177. https://doi.org/10.19044/esj.2018.v14n27p157

Omoruyi, D.I., Ilevbare, M., Ehinlaiye, A.O., and Akujieze, C.N., 2022. Geochemical discriminant for provenance characterization of some clay deposits in Edo State, Nigeria. International Journal of Earth Sciences Knowledge and Applications, 4(3), Pp. 407–418.

Oti, C.F., and Nwachukwu, A.E., 2021. Petrographic and geochemical evidence for provenance, paleo-weathering and tectonic setting of the Maastrichtian–Palaeocene sandstones from Anambra Basin, southeast Nigeria. Journal of African Earth Sciences, 179, Article ID 104225. https://doi.org/10.1016/j.jafrearsci.2021.104225

Tijani, M.N., Nton, M.E., and Kitagawa, R., 2010. Textural and geochemical characteristics of Ajali Sandstone, Anambra Basin, SE Nigeria: Implications for its provenance. Comptes Rendus Geoscience, 342, Pp. 136–150.

Zhang, S., Yang, T., Sun, X., Wei, H., and Wu, Y., 2021. Geochemical characteristics and provenance of the Upper Jurassic Linxi Formation in the northeastern Junggar Basin, China: Implications for paleoclimate and paleogeography. Journal of Petroleum Science and Engineering, 202, Article ID 108596

.